Accepted Manuscript

Forced Vibration Analysis of Functionally Graded Porous Deep Beams

Şeref Doğuşcan Akbaş

PII: S0263-8223(17)32449-2
DOI: https://doi.org/10.1016/j.compstruct.2017.12.013
Reference: COST 9170

To appear in: *Composite Structures*

Received Date: 2 August 2017
Revised Date: 27 November 2017
Accepted Date: 11 December 2017

Please cite this article as: Akbaş, S.D., Forced Vibration Analysis of Functionally Graded Porous Deep Beams, *Composite Structures* (2017), doi: https://doi.org/10.1016/j.compstruct.2017.12.013

Forced Vibration Analysis of Functionally Graded Porous Deep Beams

Şeref Doğuşcan AKBAŞ

Bursa Technical University, Department of Civil Engineering,
16330, Yıldırım/Bursa, Turkey, E-mail: serefda@yahoo.com

ABSTRACT

The purpose of this study is to investigate forced vibration analysis of functionally graded porous deep beams under dynamically load. Mechanical properties of the functionally graded deep beam change in the thickness direction with porosity. The beam theories fail to satisfy in the calculation and the boundary conditions of deep beams. So, the plane solid continua model is used in the calculation of deep beams in order to obtain more realistic results. The governing equations of the problems are obtained by using the Hamilton procedure. In the solution of the problem, finite element method is used within the plane solid continua model. The effects of porosity parameters, material distribution and porosity models on the forced vibration responses of functionally graded deep beams are examined and discussed with porosity effects. Numerical results show that porosity plays very important role in the dynamic responses of the functionally graded deep beam. Choosing the suitable functionally graded material distribution, negative effects of the porosity can be decreased. It is necessary to use the plane solid continua model in modelling the deep beams.

Keywords: Forced Vibration; Functionally Graded Materials; Porosity; Deep Beams; Finite Element Method.

1. INTRODUCTION

During the processing in the fabrication of functionally graded materials, it can occur micro-voids and porosities in the material body due to technically problems, curing or poor quality productions. Especially, the part of ceramic in the functionally graded materials occurs voids more frequently. It is known that the porosity is defined a measure of voids, and is a fraction of the volume of voids on the total volume. The volume of voids over the total volume varies between 0 and 1. The porosity is very important issue in the mechanical behavior of structures because materials can lose their strength after a certain porosity ratio. Therefore, understanding the mechanical behavior of structural elements with porosity is importance in designs.

In the present study, the forced vibration of a functionally graded deep beam under dynamically load studied with porosity effect. In the literature, much more attention has been given to the vibration analysis of functionally graded beam structures (Chakraborty et al. [1], Lu and Chen [2], Aydogdu and Taskin [3], Ying et al. [4], Li et al. [5], Azadi [6], Alshorbagy et al. [7], Fallah and Aghdam [8], Şimşek et al. [9], Akgöz and

Civalek [10,11], Akbaş [12,13,14], Zahedinejad [15], Zamanzadeh et al. [16], Bourada et al. [17], Mohanty et al. [18], Ebrahimi et al. [19], Mohanty et al. [20], Satouri et al. [21], Ebrahimi and Dashti [22], Hadji and Bedia [23], Khan et al. [24], Bennai et al. [25], Jahwari and Naguib [26], Ebrahimi et al. [27], Akgöz and Civalek [28], Sayyad et al. [29], Bounouara et al. [30], Bouafia et al. [31], Hebali et al. [32], Meziane et al. [33], Mahi and Tounsi [34], Boukhari et al. [35], Besseghier et al. [36], Bellifa et al. [37], Akbaş [38,39,40,41], Bouderba et al. [42], Zidi et al. [43] , Bennoun et al. [44], Belabed et al. [45]). However, mechanical behaviors of functionally graded deep beams have not been broadly investigated. In the open literature, studies of functionally graded deep beams are as follows; Sahraee and Saidi [46] investigated buckling and vibration of functionally graded deep beams. Shahsiah vd. [47] and Sabzikar Boroujerdy and Eslami [48] studied thermal instability of functionally graded deep spherical shells. Kurtaran [49] investigated large deflections of functionally graded deep curved beams by using generalized differential quadrature method. Hosseini and Rahmani [50] studied vibration of functionally graded deep curved nanobeams by using Navier method within Timoshenko beam theory. Ye et al. [51] investigated three-dimensional (3D) vibration of functionally graded sandwich deep beams. Pandit et al. [52] investigated wave propagation of functionally graded layers over porous half-space.

In the literature, studies of the porosity effect in the functionally graded structures are as follows; Wattanasakulpong and Ungbhakorn [53] examined vibration analysis of functionally graded beams with porosity effects. Mechab et al. [54,55] examined dynamics of a functionally graded porous nano-plate resting on foundations. Atmane et al. [56] studied vibration of functionally graded beams with different beams theories. Chen et al. [57] investigated bending and buckling of functionally graded beams. Şimşek and Aydın [58] examined forced vibration of functionally graded microplates with porosity effects based on the modified couple stress theory. Vibration characteristics of functionally graded beams with porosity effect and various thermal and mechanical loadings are investigated by (Ebrahimi and Jafari [59], Yahia et al. [60], Atmane et al. [61], Akbaş et al. [62,63,64]). Chen et al. [65] investigated free and forced vibration analysis of functionally graded porous beams within Timoshenko beam theory and Ritz method. Barati et al. [66] examined the buckling of functionally graded piezoelectric plates with porosity effect.

In the open literature, forced vibration of functionally graded porous deep beams has not been investigated broadly. The main purpose of this study is to fill this gap for functionally graded deep beams. Another distinctive feature of this study is the using the plane solid continua model which is greatly superior to the beam theories in order to obtain more realistic results for the beam. The considered problem is solved by using the finite element model of plane piecewise solid continua. In the finite element model, twelve-node plane element is used. Five-point Gauss rule is used in the numerical calculation. The effects of material parameters and porosity parameters on the forced vibration responses functionally graded deep beams are investigated with different porosity models. Also, the difference between of the porosity models is investigated in detail.

2. THEORY AND FORMULATION

A simply supported functionally graded deep beam a dynamically distributed load $q(t)$ as shown in figure 1 according to coordinate system (X, Y, Z) that L is length, b is width and h is height.

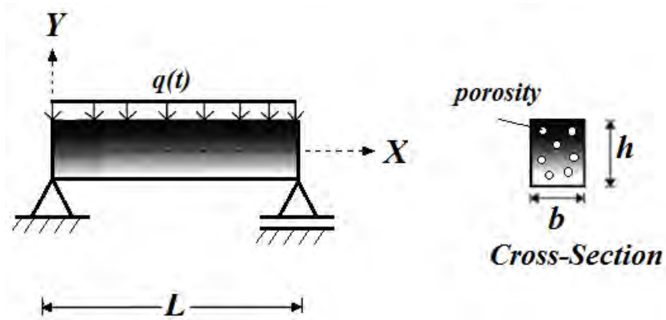

Figure 1. A simply supported functionally graded deep beam with porosity subjected dynamic distributed load.

The mechanical properties of the functionally graded deep beam, P, are assumed varying along the height direction with the following function (a power-law):

$$P(Y) = (P_T - P_B)\left(\frac{Y}{h} + \frac{1}{2}\right)^n + P_B \quad (1)$$

where n is the volume fraction index which defines the material distribution through Y direction, P_T and P_B are the material properties of the top and the bottom surfaces of the functionally graded deep beam. The functionally graded deep beam becomes a fully top surface material when n is set to zero. In the porosity effect of the functionally graded deep beam, two porosities models (even and uneven) are used which given by Wattanasakulpong and Ungbhakorn [53] for the power law distribution. In the even porosity model, the porosity spread uniformly though height direction. In the uneven porosity model, the porosity spread functionally though height direction. The distributions of the even and uneven porosity distributions are shown in Figure 2.

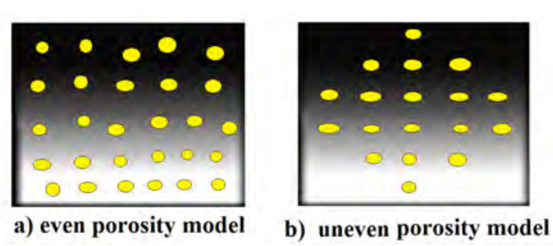

Figure 2. Porosity models for functionally graded material.

For the even porosity model, the effective material property given as follows

$$P(Y,a) = (P_T - P_B)\left(\frac{Y}{\square} + \frac{1}{2}\right)^n + P_B - (P_T + P_B)a \tag{2}$$

where a (a<<1) is the volume fraction of porosities. When a=0 , the beam becomes perfect functionally graded material. The effective material property of uneven porosity distribution can be expressed in the equation (3).

$$P(Y,a) = (P_T - P_B)\left(\frac{Y}{\square} + \frac{1}{2}\right)^n + P_B - (P_T + P_B)\frac{a}{2}\left(1 - \frac{2|Y|}{h}\right) \tag{3}$$

In the comparison of the two porosity models: In uneven porosity model, the voids stack in the neutral of the beam. So, the stiffness of the beam is less effected from negative influences of the porosity because the neutral axis and its adjacent areas have low stress. However, voids stack uniformly in the whole area of the beam in even porosity model. Hence, the stiffness of the cross-section seriously decreases in the even model. As result, the rigidity of the beam in even porosity model is lower than the rigidity of the beam in uneven porosity model.

In the solution of the functionally graded deep beam, the plane model is used in order to obtain more realistic results. It is known that the dimensions (Length and height) of the deep beams close to each other. So, the beam theories fail to satisfy in the calculation of deep beams. Also, the boundary conditions of the deep beams can not be satisfied in the beam theories. Therefore, the plane elasticity model must be considered in the deep beams.

For the plane elasticity problem, the strain- displacement relations are expressed as;

$$\varepsilon_{XX} = \frac{\partial u}{\partial X},\ \ \varepsilon_{YY} = \frac{\partial v}{\partial Y},\ 2\varepsilon_{XY} = \frac{\partial u}{\partial Y} + \frac{\partial v}{\partial X} \tag{4}$$

where u, v are displacements in the X and Y directions respectively. ε_{XX} and ε_{YY} are normal strains and ε_{XY} is shear strain. The strain- displacement relations for linear elastic material given in matrix form as follows:

$$\begin{Bmatrix} \varepsilon_{XX} \\ \varepsilon_{YY} \\ 2\varepsilon_{XY} \end{Bmatrix} = \begin{bmatrix} \frac{\partial}{\partial X} & 0 \\ 0 & \frac{\partial}{\partial Y} \\ \frac{\partial}{\partial Y} & \frac{\partial}{\partial X} \end{bmatrix} \begin{Bmatrix} u \\ v \end{Bmatrix} \tag{5}$$

$$\{\varepsilon\} = [D]\{d\} \tag{5b}$$

where $[D]$ is the differential operator between deformation and displacement, $\{d\}$ is the displacement vector. The constitutive relation of the problem is given as follows;

$$\begin{Bmatrix} \sigma_{XX} \\ \sigma_{YY} \\ \sigma_{XY} \end{Bmatrix} = \begin{bmatrix} C_{11}(Y,a) & C_{12}(Y,a) & 0 \\ C_{12}(Y,a) & C_{22}(Y,a) & 0 \\ 0 & 0 & C_{66}(Y,a) \end{bmatrix} \begin{Bmatrix} \varepsilon_{XX} \\ \varepsilon_{YY} \\ 2\varepsilon_{XY} \end{Bmatrix} \tag{6a}$$

$$\{\sigma\} = [C]\{\varepsilon\} \tag{6b}$$

where $[C]$ is the reduced constitutive tensor, and its components C_{11}, C_{12}, C_{22}, C_{66} that a function of Y and a according to equations 2 and 3 are given as follows;

$$C_{11}(Y,a) = C_{22}(Y,a) = \frac{E(Y,a)}{1-\nu(Y,a)^2}\,,\ C_{12}(Y,a) = C_{21}(Y,a) = \nu(Y,a)\frac{E(Y,a)}{1-\nu(Y,a)^2}\,,\ \ C_{66}(Y,a) = \frac{E(Y,a)}{2(1+\nu(Y,a))} \qquad (7)$$

where E and ν indicate Young's modulus and Poisson's ratio respectively.

In the deriving the governing equations of the problem, the Hamilton's procedure is used. The virtual work equation of the plane solid continua model with dynamic effect is given as follows;

$$b\int_A (\sigma_{XX}\delta\varepsilon_{XX} + 2\sigma_{XY}\delta\varepsilon_{XY} + \sigma_{YY}\delta\varepsilon_{YY} + \rho(Y,a)\ddot{u}\delta u + \rho(Y,a)\ddot{v}\delta v)dA - b\int_S (r_X\delta u + r_Y\delta v)dS$$

$$-b\int_A (k_X\delta u + k_Y\delta v)\, dA = 0 \qquad (8)$$

ρ is the mass density, r_X and r_Y are the boundary forces in the X and Y directions respectively. k_X and k_Y are the body forces in the X and Y directions respectively. In equation 8, $\ddot{u}$ and $\ddot{v}$ indicate the second derivative with respect to time. In the finite element solution, Twelve-node plane element is used as shown in Figure 3.

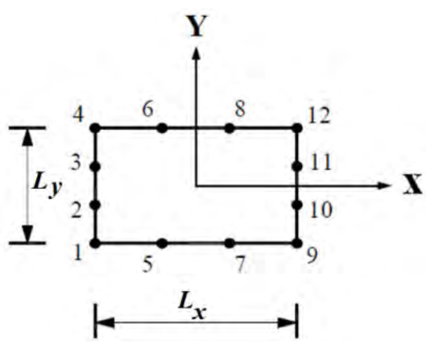

Figure 3. Twelve -node plane element.

In figure 3, L_x and L_y indicate the finite element length in the horizontal and vertical directions respectively. The displacement vector in terms of the node displacements are expressed as:

$$\{d\} = [\emptyset]\{d_n\} \qquad (9a)$$

$$[\emptyset] = [\emptyset_1\ \emptyset_2 \ldots . \emptyset_{12}] \qquad (9b)$$

$$\{d_n\} = \begin{Bmatrix} u_1 \\ u_2 \\ . \\ . \\ u_{12} \\ v_1 \\ v_2 \\ . \\ . \\ v_{12} \end{Bmatrix} \qquad (9c)$$

$$u = (u_1\emptyset_1 + u_2\emptyset_2 + u_3\emptyset_3 + u_4\emptyset_4 + u_5\emptyset_5 + u_6\emptyset_6 + u_7\emptyset_7 + u_8\emptyset_8 + u_9\emptyset_9 + u_{10}\emptyset_{10}$$

$$+u_{11}\emptyset_{11} + u_{12}\emptyset_{12}) \tag{9d}$$

$$v = (v_1\emptyset_1 + v_2\emptyset_2 + v_3\emptyset_3 + v_4\emptyset_4 + v_5\emptyset_5 + v_6\emptyset_6 + v_7\emptyset_7 + v_8\emptyset_8 + v_9\emptyset_9 + v_{10}\emptyset_{10}$$

$$+v_{11}\emptyset_{11} + v_{12}\emptyset_{12}) \tag{9e}$$

where $\{d_n\}$ is the node displacement vector and its components are u_i and v_i. $\emptyset_i$ indicates the shape functions which given for twelve-node plane element as follows;

$$\emptyset_1 = \frac{1}{32}\left(1-\frac{2X}{L_x}\right)\left(1-\frac{2Y}{L_y}\right)\left(-10+9\left(\frac{4X^2}{{L_x}^2}+\frac{4Y^2}{{L_y}^2}\right)\right),\ \emptyset_2 = \frac{9}{32}\left(1-\frac{2X}{L_x}\right)\left(1-\frac{4Y^2}{{L_y}^2}\right)\left(1-\frac{6Y}{L_y}\right)$$

$$\emptyset_3 = \frac{9}{32}\left(1-\frac{2X}{L_x}\right)\left(1-\frac{4Y^2}{{L_y}^2}\right)\left(1+\frac{6Y}{L_y}\right),\quad \emptyset_4 = \frac{1}{32}\left(1-\frac{2X}{L_x}\right)\left(1+\frac{2Y}{L_y}\right)\left(-10+9\left(\frac{4X^2}{{L_x}^2}+\frac{4Y^2}{{L_y}^2}\right)\right)$$

$$\emptyset_5 = \frac{9}{32}\left(1-\frac{2Y}{L_y}\right)\left(1-\frac{4X^2}{{L_x}^2}\right)\left(1-\frac{6X}{L_x}\right),\quad \emptyset_6 = \frac{9}{32}\left(1+\frac{2Y}{L_y}\right)\left(1-\frac{4X^2}{{L_x}^2}\right)\left(1-\frac{6X}{L_x}\right)$$

$$\emptyset_7 = \frac{9}{32}\left(1-\frac{2Y}{L_y}\right)\left(1-\frac{4X^2}{{L_x}^2}\right)\left(1+\frac{6X}{L_x}\right),\quad \emptyset_8 = \frac{9}{32}\left(1+\frac{2Y}{L_y}\right)\left(1-\frac{4X^2}{{L_x}^2}\right)\left(1+\frac{6X}{L_x}\right)$$

$$\emptyset_9 = \frac{1}{32}\left(1+\frac{2X}{L_x}\right)\left(1-\frac{2Y}{L_y}\right)\left(-10+9\left(\frac{4X^2}{{L_x}^2}+\frac{4Y^2}{{L_y}^2}\right)\right),\quad \emptyset_{10} = \frac{9}{32}\left(1+\frac{2X}{L_x}\right)\left(1-\frac{4Y^2}{{L_y}^2}\right)\left(1-\frac{6Y}{L_y}\right)$$

$$\emptyset_{11} = \frac{9}{32}\left(1+\frac{2X}{L_x}\right)\left(1-\frac{4Y^2}{{L_y}^2}\right)\left(1+\frac{6Y}{L_y}\right),\quad \emptyset_{12} = \frac{1}{32}\left(1+\frac{2X}{L_x}\right)\left(1+\frac{2Y}{L_y}\right)\left(-10+9\left(\frac{4X^2}{{L_x}^2}+\frac{4Y^2}{{L_y}^2}\right)\right) \tag{10}$$

Substituting equations (5b), (11) and (13) into equation (6), the constitutive relation can be rewritten as follows:

$$\{\sigma\} = [C][D][\emptyset]\{d_n\}=[C][B]\{d_n\} \tag{11}$$

where

$$[B] = [D][\emptyset] \tag{12}$$

The virtual displacements and virtual strains can be expressed in matrix as follows:

$$\{\delta d\} = [\emptyset]\{\delta d_n\},\quad \{\delta\ddot{d}\} = [\emptyset]\{\delta\ddot{d_n}\},\quad \{\delta\varepsilon\} = [B]\{\delta d\} \tag{13}$$

Substituting equations (5) and (9) into equation (8), the virtual work equation can be rewritten as follows;

$$b\int_A \{\delta d_n\}^T\left([B]^T[C][B]\{d_n\} + \rho(Y,a)[\emptyset]^T[\emptyset]\{\delta\ddot{d}\}\right)dA$$

$$\text{-}b\int_S \{\delta d_n\}^T[\emptyset]^T\begin{Bmatrix} r_X \\ r_Y \end{Bmatrix}dS - b\int_A \{\delta d_n\}^T[\emptyset]^T\begin{Bmatrix} k_X \\ k_Y \end{Bmatrix}dA = 0 \tag{14a}$$

$$\{\delta d_n\}^T\left([K]\{d_n\} + [M]\{\ddot{d}\} - \{r\} - \{s\}\right) = 0 \tag{14b}$$

In equation (14b), δd_n is an arbitrary values. So, the parenthesis in equation (14b) should be zero and gives the equation of motion:

$$[K]\{d_n\} + [M]\{\ddot{d_n}\} = \{F\} \tag{15}$$

where $[K]$ is element stiffness matrix, $[M]$ is the element mass matrix, $\{F\}$ is the load vector, $\{d_n\}$ is the displacement vector, $\{\ddot{d}_n\}$ is the acceleration vector, $\{s\}$ is the body force vector, $\{r\}$ is the surface load vector. The details of components of the finite element equation are given as follows:

$$[K] = b\int_A [B]^T[C][B]dA \tag{16a}$$

$$[M] = b\int_A \rho(Y,a)[\emptyset]^T[\emptyset]dA \tag{16b}$$

$$\{F\} = \{r\} + \{s\} \tag{16c}$$

$$\{r\} = \int_S [\emptyset]^T \begin{Bmatrix} r_X \\ r_Y \end{Bmatrix} dS \tag{16d}$$

$$\{s\} = \int_A [\emptyset]^T \begin{Bmatrix} k_X \\ k_Y \end{Bmatrix} dA \tag{16e}$$

Implementing assembly procedure for the finite elements, the system stiffness and mass matrixes are obtained from the element stiffness and mass matrixes. The dimension of the finite element matrixes are equal to the number of the freedom degree. For the forced vibration problem, the distributed dynamic load is considered as a harmonic function as follows;

$$q(t) = q_0 \sin(\overline{w}t) \tag{17}$$

where q_0 is the amplitude of the dynamic load and $\overline{w}$ is the frequency of the dynamic load. In the solution of the forced vibration problem, the displacement vector is assumed according to the property of the dynamic load as following form:

$$\{d_n\} = \{d_m\}\sin(\overline{w}t) \tag{18}$$

where $\{d_m\}$ indicates the amplitude of the displacements. Substituting the equation (18) into the equation (15), the equation of motion in the finite element model can be rewritten in the steady-state form as follows;

$$\{d_m\}([K] - \overline{w}^2[M]) = \{F\} \tag{19}$$

For the free vibration problem, the load vector $\{F\}$ is set to zero in the equation (15) and lead to the following an eigenvalue problem:

$$[K]\{d_n\} + [M]\{\ddot{d}\} = 0 \tag{20a}$$

$$([K] - \omega^2[M])\{\hat{d}_n\} = 0 \tag{20b}$$

where ω is the fundamental frequency and $\hat{d}_n$ is the mode vector.

3. NUMERICAL RESULTS

In the numerical examines, the forced vibration responses of the simply supported functionally graded deep beam are calculated and presented in figures in the steady-state case for different porosity parameters, porosity models and material distributions. The difference between of the porosity models is investigated. The functionally graded porous deep beam considered is made of Aluminum (Al; E=70 GPa, ν=0.3, ρ=2702 kg/m^3) and Zirconia (E=151GPa, ν=0.3, ρ=3000 kg/m^3) in numerical examples. The top surface material of the functionally graded deep beam is Zirconia, the bottom surface material of the functionally graded deep beam is Aluminum. The dimensions of the deep beam are considered as follows: b = 0.2 m, h = 2 m, L = 4 m. In numerical process, five-point Gauss rule is used for calculation of the integration.

In order to obtain the optimum number of the finite element for the numerical calculations, the convergence study is performed in figure 4. In figure 4, the maximum vertical displacements (at the middle of the beam) of the functionally graded porous deep beam are calculated for different numbers of finite elements, the power-law exponent n=3, the porosity parameter a=0.2 for even porosity model for the amplitude of the dynamic load $q_0 = 200000\ kN/m$ and the frequency of the dynamic load $\overline{w}$=2 rd/sn. It is noted that the finite element of the functionally graded deep beam is chosen to be equal in X and Y directions in order to obtain sensitive results. In figure 4, m_X and m_Y indicate the number of finite element in X and Y directions, respectively. Figure 4 shows that the dimensionless fundamental frequencies converge perfectly after the finite element m_X = m_Y =30. So, the finite element number is taken as 30 in both X and Y directions.

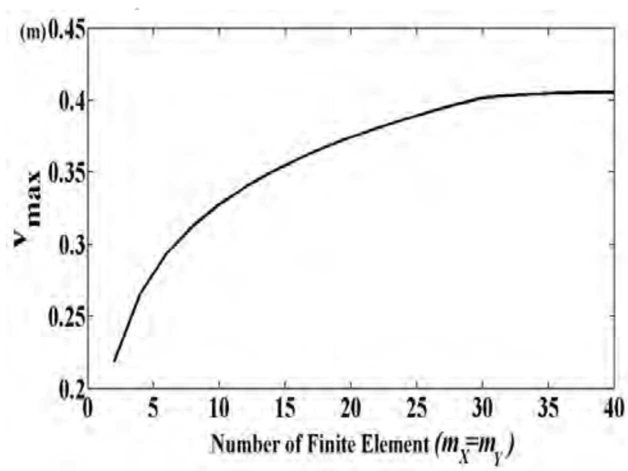

Figure 4. Convergence study for the maximum vertical displacements (v_{max}) of the functionally graded porous deep beam.

In order to confirm the accuracy of presented method, a validation study is presented. In the validation study, the dimensionless fundamental frequencies ($\overline{\boldsymbol{\omega}} = \omega\sqrt{\rho_B L^4 / E_B h^2}$) with different porosity parameters a, material distrubition parameters n and different porosity models are calculated and compared with those of Ebrahimi and Jafari [59] according to Reddy beam theory in Table 1. The material and geometry parameter are used in

Ebrahimi and Jafari [59]; steel (bottom surface) and silicon nitride (top surface), *L/h*=20 for the material properties without temperature effect (*ΔT=0*). It is seen from table 1, the present results are close to the results of Ebrahimi and Jafari [59].

Table 1. Comparison study: dimensionless fundamental frequencies of porous simple supported beam for *L/h*=20.

Porosity Models	*a*	*n*=0.5		*n*=2	
		Present	Ebrahimi and Jafari [59]	Present	Ebrahimi and Jafari [59]
Even model	0	4.52911	4.51585	3.5661	3.55529
	0.1	4.5953	4.58213	3.5202	3.50825
	0.2	4.6761	4.66783	3.4606	3.44947
Uneven model	0	4.5391	4.51585	3.5643	3.55529
	0.1	4.6182	4.60304	3.5912	3.58170
	0.2	4.7184	4.70024	3.6381	3.61002

In figure 5, the effect of the material distribution parameter n on the maximum vertical displacements (at the middle of the beam) of the porous functionally graded deep beam is presented for different porosity parameters and porosity models for $q_0 = 200000\ kN/m$ and $\overline{w}$=10 *rd/sn*. It is obvious from this figure that increasing the material distribution parameter n yields increasing of the maximum vertical displacements for all porosity models. With increase in the *n*, the beam gets to fully Aluminum according to equation (2-3). The Young modulus of the Zirconia Oxide is bigger than Aluminum. As it is expected, with increase the *n,* the elasticity modulus and bending rigidity of the beam decrease according to equation (2) and (3). So, the strength of material decreases and the displacements increases naturally. Another result of the figure 5 that with increase the material distribution parameter *n*, the difference between of porosity models increases considerably. The material distribution parameter *n* is very effective in the porosity. It is seen from figure 5 that the increase in porosity parameter *a* causes increase in the displacements significantly. It is known that increase in the porosity, the strength of the material decreases and the displacements of the beam increase naturally because of increasing voids. With these negative effects of the porosity, the strength of beam may be lost after a certain value of porosity parameter. In figure 5, the displacements decrease with decreasing the material distribution parameter *n* as the porosity parameter *a* is keep constant. The negative effects of the porosity on the functionally graded structures can be reduced with the suitable choice of material distribution parameter.

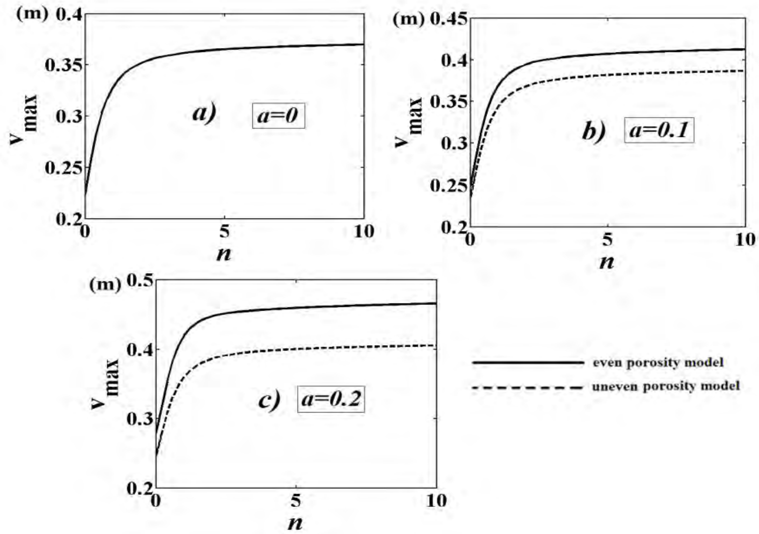

Figure 5. The relationship between of the maximum vertical displacements (v_{max}) and the material distribution parameter n for different porosity models and parameters for a) a=0, b) a=0.1 and c) a=0.2.

Figure 6 displays the relationship between of porosity parameter a and the maximum vertical displacements of the functionally graded porous deep beam for the different material distribution parameters and porosity models for $q_0 = 200000\ kN/m$ and $\overline{w}$=10 *rd/sn.* It is observed from figure 6 that the results of the even porosity model are bigger than the in uneven porosity model's. It is mentioned before that, the rigidity of the beam in even porosity model is lower than the rigidity of the beam in the uneven porosity model. So, the maximum vertical displacements in even porosity model are bigger than uneven model's. Also, as seen from figure 6 that increase in the porosity parameter a, the difference between of porosity models increases considerably. In higher values of porosity parameter a, the difference of porosity models is quite large. It shows that the porosity parameters play a critical role on the mechanical behavior of the functionally graded porous deep beam.

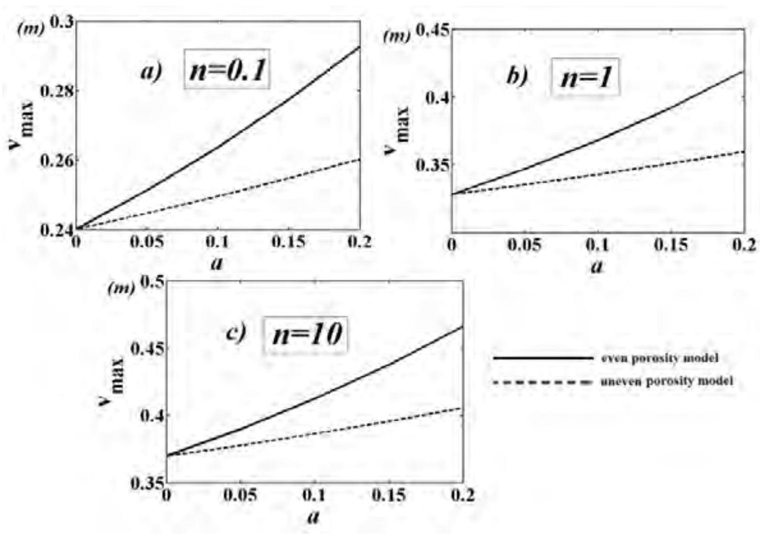

Figure 6. Effect of porosity parameter (a) and porosity models on of the maximum vertical displacements (v_{max}) of the functionally graded porous beam for different the material distribution parameter; a) $n=0.1$, b) $n=1$ and c) $n=10$.

Figure 7 and figure 8 display the relationship between the frequency of the dynamic load ($\overline{w}$) and maximum vertical displacements of the functionally graded porous deep beam for porosity parameter and material distribution parameter respectively, for $q_0 = 200000\ kN/m$ for different porosity models.

As seen from figure 7 and 8 that, the displacements rise suddenly at the resonance points where the frequency of the dynamic load ($\overline{w}$) equal to the fundamental frequency of the beam. It is observed from figure 7 and 8 that the resonance frequency in the uneven porosity model is bigger than the resonance frequency in the even porosity model. It is stated before that the functionally graded deep beam is more less strength in even porosity model in comparison with uneven model. Hence, the resonance frequency in even porosity model are smaller than uneven model's.

In figure 7, the peak of the resonance increases with increase in the porosity parameters. It is observed from figure 7 that the peak value of the resonance in the uneven porosity parameter is bigger than the peak value of the even'. Also, the difference between of even and uneven porosity models in the peak value of the resonance increase significantly with increased porosity.

In figure 8, the peak value of the resonance in the even porosity parameter is bigger than the peak value of the uneven' in the small values of *n*. With increased the material distribution parameter *n* up to a certain value, the difference between of even and uneven porosity models decrease. In the higher values of *n*, the peak value of the resonance in the uneven porosity parameter is bigger than the peak value of the even'. Another results of the figure 8 that the resonance frequency decrease significantly with increased the material distribution parameter *n*. It is concluded from figure 7 and 8 that the porosity parameter *a* and the material distribution parameter *n* play a important role on the resonance of the functionally graded porous deep beams.

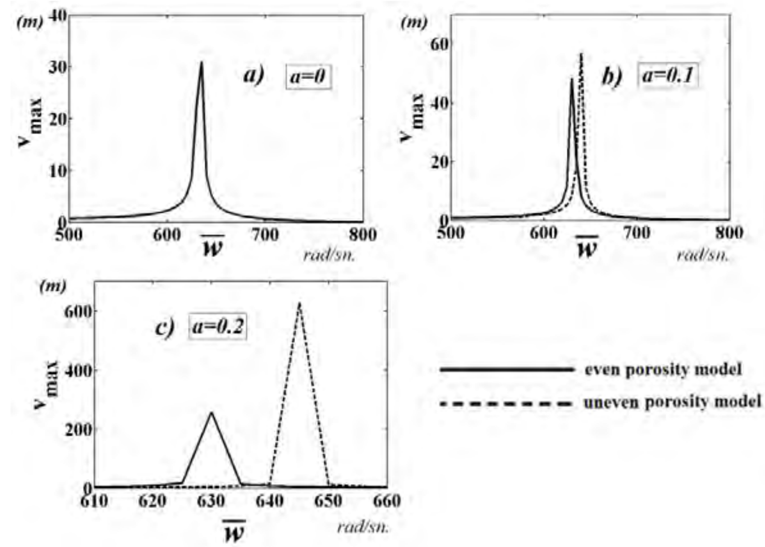

Figure 7. The relationship between of the maximum vertical displacements (v_{max}) and the frequency of the dynamic load ($\overline{w}$) for different porosity parameters and models for n=3 for a) a=0, b) a=0.1 and c) a=0.2.

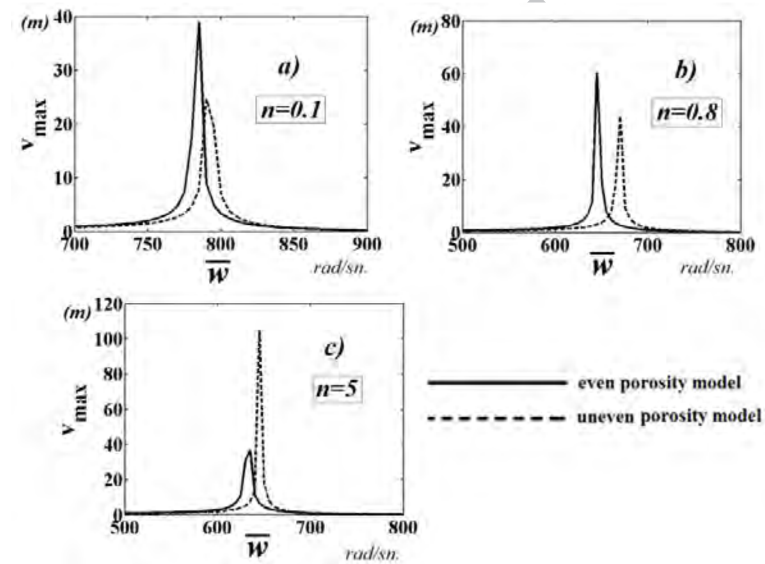

Figure 8. The relationship between of the maximum vertical displacements (v_{max}) and the frequency of the dynamic load ($\overline{w}$) for different material distribution parameters and porosity models for a=0.2 for a) n=0.1, b) n=0.8 and c) n=5.

Figure 9 shows that the effect of parameter a on the deflected shape of the functionally graded porous deep beam for even porosity model for $q_0 = 400000\ kN/m$, $\overline{w}$=500 *rd/sn* and n=0.6. It is seen from figure 9 that the deflections of the functionally graded deep beam increase significantly with increase in the a.

In figure 10, the effect of parameter a on the time responses of the functionally graded porous deep beam are shown for different porosity parameters and models for $q_0 = 200000\ kN/m$, $\overline{w}$=3 *rd/sn* and n=2. As seen from figure 10 that the difference between of even and uneven porosity models in the time responses increase with increase in the porosity parameter a.

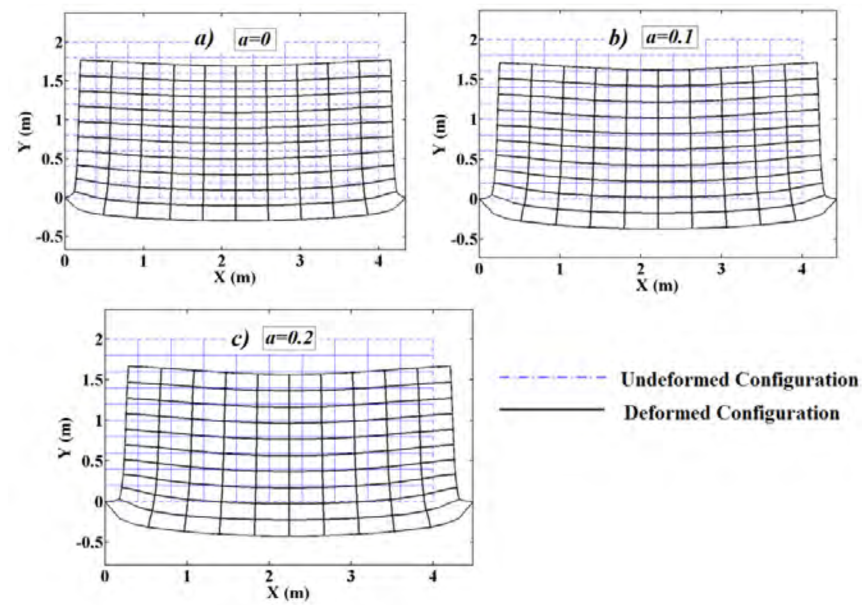

Figure 9. The effect of porosity parameter *a* on the deflected shape of the functionally graded porous deep beam for a) *a*=0, b) *a*=0.1 and c) *a*=0.2.

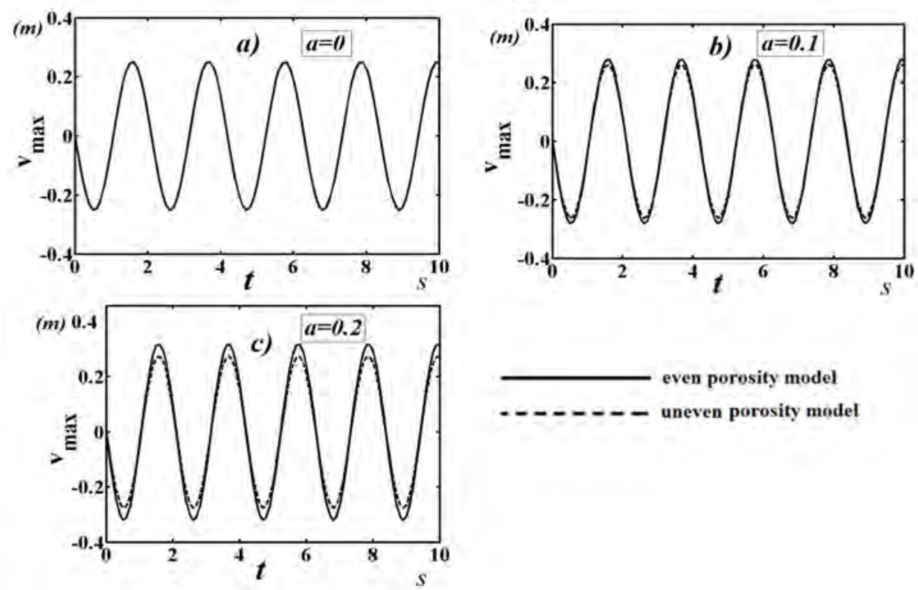

Figure 10. Time responses of the functionally graded porous deep beam for; a) *a*=0, b) *a*=0.1 and c) *a*=0.2.

In order to investigate the effects of the aspect ratios (*L/h*) on the dynamic responses of the functionally graded porous beams, the maximum vertical displacements are presented for different aspect ratios, porosity parameters and porosity models for $q_0 = 100000\ kN/m$, *n*=0.1 and $\overline{w}$=10 *rd/sn* in figure 11. It is seen from figure 11 that the increase in the aspect ratios (*L/h*) causes increase in the difference between even and uneven porosity models significantly. This difference becomes more apparent in higher aspect ratios and porosity parameters. The porosity is more effective in the higher aspect ratios in comparison with the smaller aspect ratios, namely deep or thick beams.

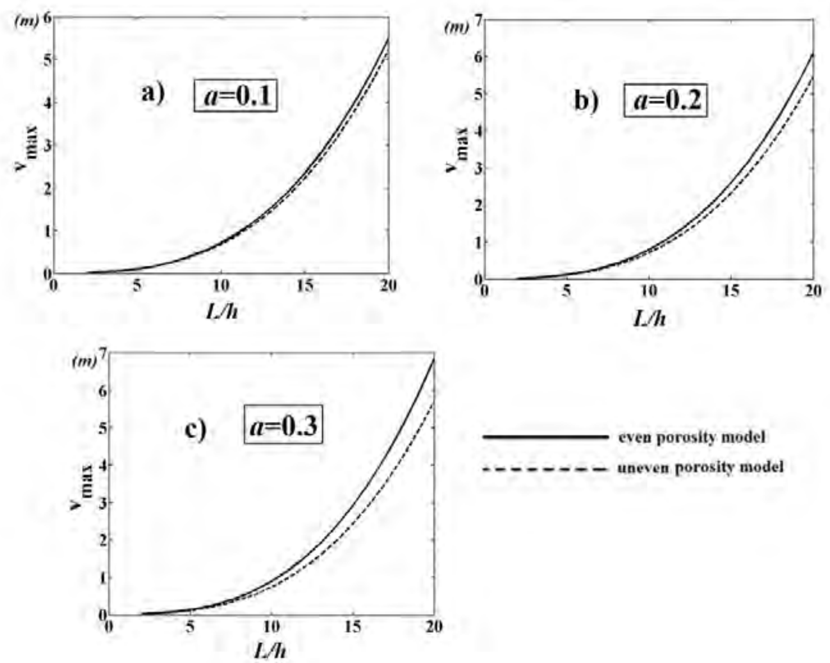

Figure 11. The relationship between of the maximum vertical displacements (v_{max}) and the aspect ratios (L/h)for different porosity models and parameters for a) a=0.1, b) a=0.2 and c) a=0.3.

4. CONCLUSIONS

Forced vibration of a functionally graded deep beam are investigated with porosity effect under a harmonic external distributed load by using the finite element method. In solution modeling of the problem, the plane piecewise solid continua model is implemented. The effects of porosity parameters, material distribution and porosity models on the forced vibration responses of the functionally graded deep beam are investigated. It is observed from the investigations, the main conclusions are as follows:

- The porosity has a very important role on the dynamic of the functionally graded deep beam.
- Increase in the porosity parameter a, the difference between the porosity models increases considerably.
- It is necessary to use the plane solid continua model in modelling the deep beams in order to obtain more realistic results.
- The material distribution plays determining role on the forced vibration responses of the porous functionally graded deep beam.
- Choosing the suitable material distribution parameter, harmful effects of the porosity can be decreased.

REFERENCES

1. Chakraborty A, Gopalakrishnan S and Reddy JN. A new beam finite element for the analysis of functionally graded materials. International Journal of Mechanical Sciences 2003; 45(3):519-539.
2. Lu CF and Chen WQ. Free vibration of orthotropic functionally graded beams with various end conditions. Structural Engineering and Mechanics 2005;20(4): 465-476.
3. Aydogdu M and Taskin V. Free vibration analysis of functionally graded beams with simply supported edges. Materials & design 2007;28(5): 1651-1656.
4. Ying J, Lü CF, and Chen WQ. Two-dimensional elasticity solutions for functionally graded beams resting on elastic foundations. Composite Structures 2008;84(3):209-219.
5. Li SR, Su HD and Cheng CJ. Free vibration of functionally graded material beams with surface-bonded piezoelectric layers in thermal environment. Applied Mathematics and Mechanics 2009;30(8) : 969-982.
6. Azadi M. Free and forced vibration analysis of FG beam considering temperature dependency of material properties. Journal of Mechanical Science and Technology 20112;5(1) : 69-80.
7. Alshorbagy AE, Eltaher MA and Mahmoud FF. Free vibration characteristics of a functionally graded beam by finite element method. Applied Mathematical Modelling 20113;5(1): 412-425.
8. Fallah A and Aghdam MM. Thermo-mechanical buckling and nonlinear free vibration analysis of functionally graded beams on nonlinear elastic foundation. Composites Part B: Engineering 2012;43(3) : 1523-1530.
9. Şimşek M, Kocatürk T and Akbaş ŞD. Dynamic behavior of an axially functionally graded beam under action of a moving harmonic load. Composite Structures 2012;94(8) :2358-2364.
10. Akgöz B and Civalek Ö. Shear deformation beam models for functionally graded microbeams with new shear correction factors. Composite Structures 2014; 112: 214-225.
11. Akgöz B and Civalek Ö. Free vibration analysis of axially functionally graded tapered Bernoulli–Euler microbeams based on the modified couple stress theory. Composite Structures 2013;98: 314-322.
12. Akbaş ŞD. Free vibration characteristics of edge cracked functionally graded beams by using finite element method, International Journal of Engineering Trends and Technology 2013; 4(10):4590-4597.
13. Akbaş ŞD. Free vibration of axially functionally graded beams in thermal environment. International Journal of Engineering and Applied Sciences 2014;6(3): 37-51.
14. Akbaş ŞD. Free vibration of edge cracked functionally graded microscale beams based on the modified couple stress theory. International Journal of Structural Stability and Dynamics 2016;17(03): 1750033.
15. Zahedinejad P. Free vibration analysis of functionally graded beams resting on elastic foundation in thermal environment. International Journal of Structural Stability and Dynamics 2016;16(07):1550029.
16. Zamanzadeh M, Rezazadeh G, Jafarsadeghi-Pournaki I and Shabani R. Thermally induced vibration of a functionally graded micro-beam subjected to a moving laser beam. International Journal of Applied Mechanics 2014;6(06) :1450066.

17. Bourada M, Kaci A, Houari MSA and Tounsi A. A new simple shear and normal deformations theory for functionally graded beams. Steel and composite structures 2015;18(2) : 409-423.

18. Mohanty SC, Dash RR and Rout T. Vibration and Dynamic Stability of Pre-Twisted Thick Cantilever Beam Made of Functionally Graded Material. International Journal of Structural Stability and Dynamics, 2015;15(04):1450058.

19. Ebrahimi F, Salari E, and Hosseini SAH. Thermomechanical vibration behavior of FG nanobeams subjected to linear and non-linear temperature distributions. Journal of Thermal Stresses 2015;38(12): 1360-1386.

20. Mohanty SC, Dash RR and Rout T. Vibration and Dynamic Stability of Pre-Twisted Thick Cantilever Beam Made of Functionally Graded Material. International Journal of Structural Stability and Dynamics, 2015;15(04): 1450058.

21. Satouri S, Asanjarani A and Satouri A. Natural frequency analysis of 2D-FGM sectorial plate with variable thickness resting on elastic foundation using 2D-DQM. International Journal of Applied Mechanics 2015;7(2):1550030.

22. Ebrahimi F and Dashti S. Free vibration analysis of a rotating non-uniform functionally graded beam, Steel and Composite Structures 2015;19(5):1279-1298.

23. Hadji L and Bedia EAA. Analyse of the behavior of functionally graded beams based on neutral surface position. Structural Engineering and Mechanics 2015;55(4): 703-717.

24. Khan AA, Naushad Alam M and Wajid M. Finite Element Modelling for Static and Free Vibration Response of Functionally Graded Beam. Latin American Journal of Solids and Structures 2016;13(4): 690-714.

25. Bennai R, Atmane HA and Tounsi A. A new higher-order shear and normal deformation theory for functionally graded sandwich beams. Steel and Composite Structures 2015;19(3):521-546.

26. Jahwari F and Naguib HE. Analysis and homogenization of functionally graded viscoelastic porous structures with a higher order plate theory and statistical based model of cellular distribution. Applied Mathematical Modelling 2016;40(3):2190-2205.

27. Ebrahimi F, Ghasemi F and Salari E. Investigating thermal effects on vibration behavior of temperature-dependent compositionally graded Euler beams with porosities. Meccanica 2016;51(1): 223-249.

28. Akgöz B and Civalek Ö. Bending analysis of FG microbeams resting on Winkler elastic foundation via strain gradient elasticity. Composite Structures 2015;134: 294-301.

29. Sayyad AS and Ghugal YM. A Unified Shear Deformation Theory for the Bending of Isotropic, Functionally Graded, Laminated and Sandwich Beams and Plates. International Journal of Applied Mechanics 2017;9(01): 1750007.

30. Bounouara F., Benrahou KH, Belkorissat I. and Tounsi A. A nonlocal zeroth-order shear deformation theory for free vibration of functionally graded nanoscale plates resting on elastic foundation. Steel and Composite Structures 2016;20(2): 227-249.

31. Bouafia K, Kaci A., Houari M S A, Benzair A and Tounsi A. A nonlocal quasi-3D theory for bending and free flexural vibration behaviors of functionally graded nanobeams. Smart Structures and Systems 2017;19(2):115-126.

32. Hebali H, Tounsi A, Houari MSA, Bessaim A and Bedia EAA. (2014). New quasi-3D hyperbolic shear deformation theory for the static and free vibration analysis of functionally graded plates. Journal of Engineering Mechanics 2014;140(2): 374-383.

33. Meziane MAA, Abdelaziz HH and Tounsi A. An efficient and simple refined theory for buckling and free vibration of exponentially graded sandwich plates under various boundary conditions. Journal of Sandwich Structures & Materials 2014;16(3):293-318.

34. Mahi A and Tounsi A. (2015). A new hyperbolic shear deformation theory for bending and free vibration analysis of isotropic, functionally graded, sandwich and laminated composite plates. Applied Mathematical Modelling, 2015;39(9): 2489-2508.

35. Boukhari A, Atmane HA, Tounsi, A., Adda B and Mahmoud SR. An efficient shear deformation theory for wave propagation of functionally graded material plates. Structural Engineering and Mechanics, 2016;57(5):837-859.

36. Besseghier A, Houari MSA, Tounsi A and Mahmoud SR. Free vibration analysis of embedded nanosize FG plates using a new nonlocal trigonometric shear deformation theory. Smart Structures and Systems, 2017;19(6): 601-614.

37. Bellifa H, Benrahou KH, Hadji L, Houari MSA and Tounsi A. Bending and free vibration analysis of functionally graded plates using a simple shear deformation theory and the concept the neutral surface position. Journal of the Brazilian Society of Mechanical Sciences and Engineering 2016;38(1): 265-275.

38. Akbaş ŞD. Geometrically nonlinear static analysis of edge cracked Timoshenko beams composed of functionally graded material. Mathematical Problems in Engineering, 2013, doi:10.1155/2013/871815.

39. Akbaş ŞD. On post-buckling behavior of edge cracked functionally graded beams under axial loads. International Journal of Structural Stability and Dynamics 2013;15(04): 1450065.

40. Akbaş ŞD. Post-buckling analysis of axially functionally graded three-dimensional beams. International Journal of Applied Mechanics 2015;7(03): 1550047.

41. Akbaş, Ş. D. (2016). Wave propagation in edge cracked functionally graded beams under impact force. *Journal of Vibration and Control*, *22*(10), 2443-2457.

42. Bouderba B, Houari MSA and Tounsi A. Thermomechanical bending response of FGM thick plates resting on Winkler-Pasternak elastic foundations. Steel and Composite Structures 2013;14(1): 85-104.

43. Zidi M, Tounsi A, Houari MSA and Bég OA. Bending analysis of FGM plates under hygro-thermo-mechanical loading using a four variable refined plate theory. Aerospace Science and Technology 2014;34: 24-34.

44. Bennoun M, Houari MSA and Tounsi A. A novel five-variable refined plate theory for vibration analysis of functionally graded sandwich plates. Mechanics of Advanced Materials and Structures, 2016;23(4), 423-431.

45. Belabed Z, Houari MSA, Tounsi A, Mahmoud SR and Bég OA. An efficient and simple higher order shear and normal deformation theory for functionally graded material (FGM) plates. Composites Part B: Engineering 2014;60: 274-283.

46. Sahraee S and Saidi AR. Free vibration and buckling analysis of functionally graded deep beam-columns on two-parameter elastic foundations using the differential quadrature method. Proceedings of the Institution of Mechanical Engineers, Part C: Journal of Mechanical Engineering Science 2009;223(6): 1273-1284.

47. Shahsiah R, Eslami MR and Sabzikar Boroujerdy M. Thermal instability of functionally graded deep spherical shell. Archive of Applied Mechanics 2011;81(10): 1455-1471.

48. Sabzikar Boroujerdy M and Eslami MR. Thermal buckling of piezoelectric functionally graded material deep spherical shells. The Journal of Strain Analysis for Engineering Design 2014;49(1): 51-62.

49. Kurtaran H. Large displacement static and transient analysis of functionally graded deep curved beams with generalized differential quadrature method. Composite Structures 2015;131: 821-831.

50. Hosseini SAH and Rahmani O. Free vibration of shallow and deep curved FG nanobeam via nonlocal Timoshenko curved beam model. Applied Physics A 2016;122(3) :1-11.

51 Ye T, Jin G and Su Z. Three-dimensional vibration analysis of functionally graded sandwich deep open spherical and cylindrical shells with general restraints. Journal of Vibration and Control 2016;22(15) : 3326-3354.

52. Pandit DK, Kundu S and Gupta S. Propagation of Love waves in a prestressed Voigt-type viscoelastic orthotropic functionally graded layer over a porous half-space. Acta Mechanica 2016;228(3): 1-10.

53. Wattanasakulpong N and Ungbhakorn V. Linear and nonlinear vibration analysis of elastically restrained ends FGM beams with porosities. Aerospace Science and Technology 2014;32(1):111-120.

54. Mechab I, Mechab B, Benaissa S, Serier B, Bouiadjra BB. Free vibration analysis of FGM nanoplate with porosities resting on Winkler Pasternak elastic foundations based on two-variable refined plate theories. Journal of the Brazilian Society of Mechanical Sciences and Engineering 2016;38:2193–2211.

55. Mechab B, Mechab I, Benaissa S, Ameri M and Serier B. Probabilistic analysis of effect of the porosities in functionally graded material nanoplate resting on Winkler–Pasternak elastic foundations. Applied Mathematical Modelling 2016;40(2): 738-749.

56. Atmane HA, Tounsi A, Bernard F, and Mahmoud SR. A computational shear displacement model for vibrational analysis of functionally graded beams with porosities. Steel and Composite Structures 2015;19(2):369-384.

57. Chen D, Yang J and Kitipornchai S. Elastic buckling and static bending of shear deformable functionally graded porous beam. Composite Structures 2015;133(1): 54-61.

58. Şimşek M and Aydın M. Size-dependent forced vibration of an imperfect functionally graded (FG) microplate with porosities subjected to a moving load using the modified couple stress theory. Composite Structures 2017;160:408-421.

59. Ebrahimi F and Jafari A. A Higher-Order Thermomechanical Vibration Analysis of Temperature-Dependent FGM Beams with Porosities. Journal of Engineering 2016, doi:10.1155/2016/9561504.

60. Yahia SA., Atmane HA., Houari MSA. and Tounsi A. Wave propagation in functionally graded plates with porosities using various higher-order shear deformation plate theories. Structural Engineering and Mechanics 2015; 53(6): 1143-1165.

61.Atmane H A., Tounsi A. and Bernard F. Effect of thickness stretching and porosity on mechanical response of a functionally graded beams resting on elastic foundations. International Journal of Mechanics and Materials in Design 2017; 13(1): 71-84.

62. Akbaş ŞD. Post-buckling responses of functionally graded beams with porosities. Steel and Composite Structures 2017;24(5): 579-589.

63. Akbaş ŞD. Thermal Effects on the Vibration of Functionally Graded Deep Beams with Porosity. International Journal of Applied Mechanics 2017;9(5): 1750076.

64.Akbaş ŞD. Vibration and static analysis of functionally graded porous plates. Journal of Applied and Computational Mechanics 2017;3(3): 199-207.

65. Chen D, Yang J and Kitipornchai S. Free and forced vibrations of shear deformable functionally graded porous beams. International Journal of Mechanical Sciences 2016;108: 14-22.

66. Barati MR, Sadr MH and Zenkour AM. Buckling analysis of higher order graded smart piezoelectric plates with porosities resting on elastic foundation. International Journal of Mechanical Sciences 2016;117:309-320.